Available online at www.sciencedirect.com
SCIENCE DIRECT
International Journal of Heat and Fluid Flow 26 (2005) 873–882
International Journal of HEAT AND FLUID FLOW
www.elsevier.com/locate/ijhff

PLIF and PIV measurements of the self-preserving structure of steady round buoyant turbulent plumes in crossflow

F.J. Diez [a,*], L.P. Bernal [b], G.M. Faeth [b]

[a] Rutgers, Department of Mechanical and Aerospace Engineering, The State University of New Jersey, 98 Brett Road, Piscataway, NJ 08854-8058, USA
[b] University of Michigan, Ann Arbor, MI 48109, USA

Available online 9 November 2005

Abstract

Measurements of the mean concentration of source fluid and mean velocity fields were obtained for the first time in the self-preserving region of steady round buoyant turbulent plumes in uniform crossflows using Planar-Laser-Induced-Fluorescence (PLIF) and Particle-Image-Velocimetry (PIV), respectively. The experiments involved salt water sources injected into water/ethanol crossflows within a water channel. Matching the index of refraction of the source and ambient fluids was required in order to avoid image distortion and laser intensity nonuniformities. Further experimental methods and procedures are explained in detail. The self-preserving structure properties of the flow were correlated successfully based on the scaling analysis of [Fischer, H.B., List, E.J., Koh, R.C., Imberger, J., Brooks, N.H., 1979. Mixing in Inland and Coastal Waters, Academic Press, New York, pp. 315–389]. The resulting self-preserving structure consisted of two counter-rotating vortices having their axes nearly aligned with the crossflow direction that move away from the source in the streamwise (vertical) direction due to the action of buoyancy. This alignment, was a strong function of the source/crossflow velocity ratio, u_0/v_∞. Finally, the counter-rotating vortex system was responsible for substantial increases in the rate of mixing of the source fluid with the ambient fluid compared to axisymmetric round buoyant turbulent plumes in still environments, e.g., transverse dimensions in the presence of the self-preserving counter-rotating vortex system were 2–3 times larger than the transverse dimensions of self-preserving axisymmetric plumes at similar streamwise distances from the source.

Keywords: Heat transfer; Buoyancy; Scaling; Dispersion; Turbulence

1. Introduction

Recent progress toward understanding and modeling the structure and penetration properties of round turbulent nonbuoyant puffs, starting and steady jets, and buoyant thermals, starting plumes and steady plumes in still and crossflowing unstratified uniform environments (Sangras et al., 2002; Diez et al., 2003a,b,c, 2005), were extended to consider the structure of self-preserving steady round buoyant turbulent plumes in uniform crossflows. These flows are of interest for several reasons: they have practical applications to interrupted, developing and steady nonreactive gas and liquid releases caused by process upsets, explosions and fires; they are simple classical flows that are relatively easy to interpret in order to better understand the properties of steady and unsteady buoyant turbulent flows; and they involve uncomplicated geometries having well-defined initial and boundary conditions that provide measurements useful for evaluating models of practical buoyant turbulent flows. Motivated by this, the present work will consider the structure properties of steady plumes in crossflows emphasizing self-preserving conditions.

A visualization of a typical steady turbulent plume in crossflow appears in Fig. 1. The images consist of side and top views of a typical turbulent plume in crossflow obtained when steady flow conditions have been reached. The length scales that appear on the images are appropriate for streamwise and cross stream directions. Far from the source, the trajectory of steady turbulent plumes in crossflows

* Corresponding author. Tel.: +1 732 445 3665; fax: +1 732 445 3124.
E-mail address: diez@rutgers.edu (F.J. Diez).

0142-727X/$ - see front matter © 2005 Elsevier Inc. All rights reserved.
doi:10.1016/j.ijheatfluidflow.2005.10.003

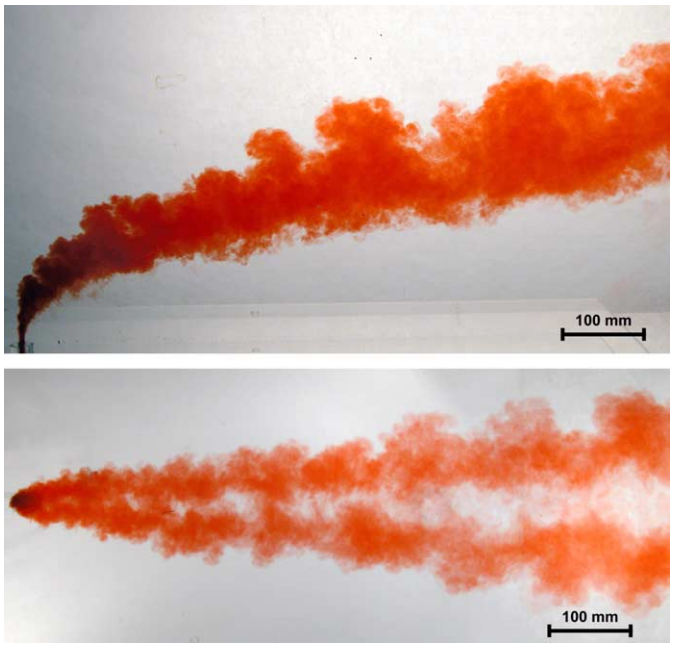

Fig. 1. Visualization of the penetration properties of a steady turbulent plume in a uniform crossflow ($d = 6.4$ mm, $Re_0 = 5{,}000$, $\rho_0/\rho_\infty = 1.150$, $Fr_0 = 223$, $u_0/v_\infty = 7$). The upper figure is a side view; the lower figure is a top view.

become nearly horizontal and self-preserving behavior is approached. When this condition is reached, the streamwise penetration of the flow approximates a two-dimensional horizontal line thermal in a still fluid. Then the streamwise motion of the line thermal, retarded along its sides in the streamwise direction by the uniform ambient crossflow, naturally leads to the flow becoming two nearly horizontal counter-rotating vortices whose axes are aligned along the axis of the plume as a whole. Evidence for this behavior is provided by the top view of the flow which is the lower image in Fig. 1, where the darker regions associated with the two vortices are separated by a significantly lighter region dominated by the presence of dye-free ambient fluid that is entrained by the vortex system along its plane of symmetry. In order to further introduce the present investigation, earlier studies of round nonbuoyant turbulent jets in still fluid will be discussed next.

Several review of earlier studies of round nonbuoyant turbulent jet flows have appeared in the literature, (see Tennekes and Lumley, 1972; Hinze, 1975; Fischer et al., 1979; List, 1982; Dahm and Dimotakis, 1990; Panchapakesan and Lumley, 1993; Mi et al., 2001 and references cited therein). Due to the availability of these references, the present discussion of the literature will be brief.

One of the simplest interactions between nonbuoyant turbulent source flows and another fluid source involves the transient development of turbulent jets in still fluids; therefore, this flow has attracted the attention of a large number of workers (e.g., see Sangras et al., 2002; Diez et al., 2003a,c; Johari and Paduano, 1987; Kato et al., 1987; Papanicolaou and List, 1988; Kouros et al., 1993, and references cited therein). Relationships for the self-preserving transient and steady penetration properties of these flows have been developed from scaling analysis and confirmed by measurements.

Most practical releases of turbulent jets and plumes are exposed to crossflow; therefore, there have been a number of attempts to extend the results just discussed for jets in still fluids to corresponding round turbulent nonbuoyant jets and buoyant plumes in uniform crossflows (see Diez et al. (2003a,b, 2005); Fischer et al. (1979); Lutti and Brzustowski, 1977; Andreopoulos, 1983; Alton et al., 1993; Baum et al., 1994; Smith and Mungal, 1998; Hasselbrink and Mungal, 2001a; Hasselbrink and Mungal, 2001b; Su and Mungal, 2004; Gordon and Soria, 2001 and references cited therein). These studies generally have shown that motion in the crossflow direction satisfies the no-slip convection approximation and that the deflection of the jet or plume toward the crossflow direction results in the development of a counter-rotating vortex system over the cross section of the flow, as discussed in connection with Fig. 1. Relationships for the self-preserving transient and steady penetration properties of these flows have been confirmed by measurements, obtaining results similar to corresponding flows in still environments. In particular, the flows become turbulent within five source diameters from the source and become self-preserving at streamwise distances greater than 40–50 source diameters from the source for $u_0/v_\infty < 35$ (Diez et al., 2003a,b, 2005). On the other hand, the rates of mixing and the structure properties of these flows at self-preserving conditions have not yet received any attention.

Based on the previous observations, the objectives of the present investigation were to extend past work concerning the self-preserving penetration properties of steady turbulent plumes in crossflows (Diez et al., 2003a,b), in order to develop an improved understanding of their self-preserving mixing structure properties, as follows:

(1) Measure the self-preserving mixing structure of these flows, including the distributions of the mean source fluid concentrations within the counter-rotating vortex system, and the distributions of the mean and velocity field, for steady flow and for source and crossflow conditions typical of practical applications.
(2) Exploit the new measurements of these flows to evaluate the effectiveness of self-preserving scaling relationships developed by Fischer et al. (1979) for flow mixing structure properties.

In order to evaluate present measurements of the flow structure, baseline measurements of the structure properties of round nonbuoyant turbulent jets in uniform still fluids were also undertaken. The present description of the research begins with a discussion of experimental methods and the self-preserving scaling properties of the flows; measured scaling results are then described, considering flow mixing structure properties.

2. Experimental methods

2.1. Test apparatus

The present experiments adopted methods analogous to the salt/fresh-water modeling experiments for buoyant turbulent flows suggested by Steckler et al. (1986). Somewhat different source and ambient fluids were required, however, because the techniques used, Planar-Laser-Induced-Fluorescence (PLIF) and Particle-Image-Velocimetry (PIV), required matching the indices of refraction of the source and ambient fluids in order to avoid scattering the laser beam away from the buoyant flow. A visual inspection of the two instantaneous PLIF images in Fig. 2 clearly shows the effect when the indices of refraction of the source and ambient fluids are not matched. Ensemble-averaged concentration contours (4000 images) taken with and without matching the index of refraction of the fluids showed concentration values up to three times higher when the index of refraction was matched which reflects the importance of index matching. A salt (potassium phosphate, monobasic KH_2PO_4) water source containing Rhodamine 6G dye was injected into an unstratified uniform ethyl alcohol/water crossflow for matched refractive index PLIF measurements of source flow concentration structure and matched refractive index PIV measurements of velocity structure. The unstratified and uniform crossflow was produced by a water channel facility. The test section of the water channel had cross section dimensions of 610×760 mm and a length of 2440 mm. Some experiments were also carried out with no water flow in order to provide observations of round nonbuoyant turbulent jets in still environments, as a baseline to evaluate methods of measuring mixing properties.

The source flows had a larger density than the crossflows for present conditions and were injected vertically downward into the channel flow to obtain steady turbulent plumes in crossflows. The source flows passed through smooth round injector tubes having inside diameters of 2.1, 3.2 and 6.4 mm. The source injector tubes had length/diameter ratios of 200, 100 and 50, respectively, to help insure fully-developed turbulent pipe flow at the source exit for sufficiently large source Reynolds numbers, as discussed by Wu et al. (1995). The source injector tubes passed through a plane horizontal Plexiglas plate (508×914 mm in plan dimension $\times$ 12 mm thick) with a tight fit. The source injector tube exits were mounted flush with the lower surface of the Plexiglas plate in order to provide well-defined entrainment conditions at the source exit. The source liquid was supplied to the tubes using either a syringe pump (Harvard Apparatus, PHD2000, Model 70–2000, with four 150 cc syringes having volumetric accuracies of $\pm 1\%$ mounted in parallel) for small flow rates, or a peristaltic pump (Masterflux L/S Digi-Staltic Dispersion, Model 72310-0) with two flow dampers for large flow rates. The pumps were calibrated by collecting liquid for timed intervals.

2.2. Structure measurements

2.2.1. Concentration measurements

The PLIF arrangement was similar to the arrangement used by Diez et al. (2005) for studies of the structure of steady turbulent jets in crossflows, except for features required to match the refractive indices of the source and crossflowing fluids discussed by Ferrier et al. (1993), Alahyari and Longmire (1994), and Daviero et al. (2001). The arrangement consisted of a laser, optics for scanning the laser beam across the image area and a digital camera for recording the image. Rhodamine 6G dye at a concentration of 5.0×10^{-6} mol/l was used for the PLIF signals in the source liquid (see Ferrier et al., 1993) for a discussion of the properties of this dye. An argon-ion laser (Coherent Innova 90-4) operated in the single-line mode at 514.5 nm with an optical power of 3200 mW and a beam diameter of 1.5 mm (at the e^{-2} intensity locations) was used to excite the fluorescence.

The use of potassium phosphate (KH_2PO_4) to increase the density of the source fluid along with an appropriate concentration of ethyl alcohol in the crossflowing water which decreased its density, matched the refractive indices of the source and ambient fluid as discussed by Ferrier et al. (1993); Alahyari and Longmire (1994); and Daviero et al. (2001). Close control of the temperature differences

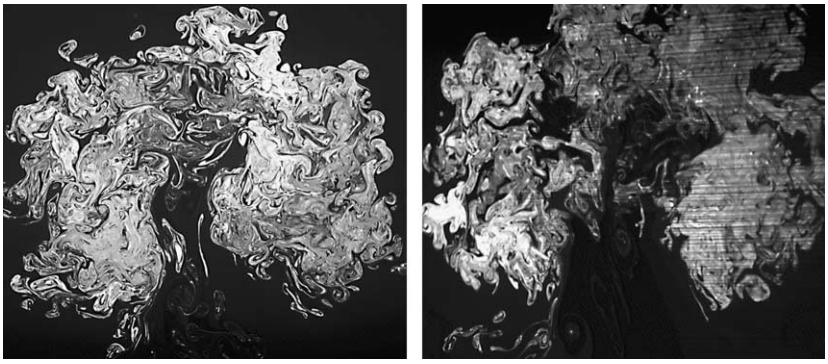

Fig. 2. Instantaneous PLIF images of the cross section of a steady turbulent plume in a uniform crossflow. Refractive index matching was done in the left image but not in the right image for comparison purposes.

between the source and ambient fluid, however, was also required for proper matching of refractive indices; this was done using a heater for the source fluid that limited temperature differences between the source and ambient fluids to less than 0.10 K.

A mirror located roughly 1000 mm downstream from the imaged cross section of the flow allowed the camera to view the PLIF image. The camera was a Redlakes Inc., Model Mega Plus ES 1020. This camera has a 1004×1004 pixel array with a 7.4×7.4 mm active sensor area. The intensity resolution of the pixels was 10-bit which provided 1024 color levels of the image. A PC-Cam Link frame grabber from Coreco Imaging transferred the camera images to a computer for processing and storage.

The digital PLIF images are individually corrected as follows:

1. The background image, which accounts for the image of mean dark current is subtracted from each image.
2. A lens calibration image shown in Fig. 3, and applied to each image, was used to remove the lens vignetting effect (Ferrier et al., 1993).
3. From simple geometry considerations it is found that the scanning laser beam produced by the oscillating mirror delivers an intensity to each point in the field of view that is dependent on the distance from that point to the oscillating mirror, the angular speed of the mirror and the reflection and transmission coefficients of the working fluids. A contour plot, shown in Fig. 4, was generated from geometrical considerations to correct for this intensity variation and applied to each image.
4. The power of the laser beam is attenuated as it passes through water, ethanol and salt. Corrections due to attenuation were done by integrating the Beer–Lambert Law (Ferrier et al., 1993; Daviero et al., 2001) as:

$$I = I_0 \exp\left(-\int_0^r a \, dr'\right), \tag{1}$$

where I_0 is the beam intensity reaching the water channel, r is the distance the light travels, I is the resulting laser intensity at that location and a is the attenuation coefficient (due to clear water, salt, ethanol and Rhodamine 6G (Daviero et al., 2001)).

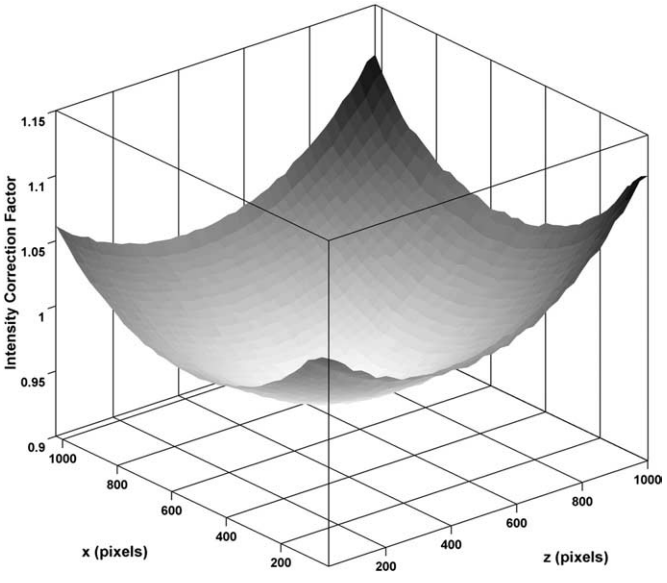

Fig. 3. Contour plot of vignetting correction image. Individual raw images are multiplied by this image to correct for vignetting effects produced by the lens used.

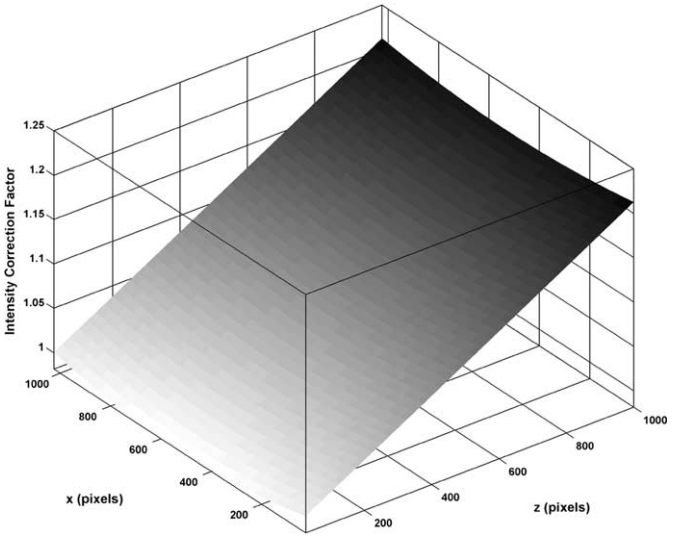

Fig. 4. This contour plot was generated from geometrical considerations to correct for beam intensity decay as a function of distance and angular speed from the scanning mirror.

Although implementing these corrections was numerically expensive, it provided results when applied to calibration images that differ by less than 1% from the actual values. Thus, they were applied to all the experimental data.

The mean concentrations of source fluid were obtained over cross sections of the flow by averaging 4000 images. The same general arrangement was used for PLIF structure measurements of round nonbuoyant turbulent jets in a still fluid in order to provide baseline results needed to evaluate the PLIF technique for measurements in crossflows. The experimental uncertainties (95% confidence) were less than 7% for mean concentrations at each point in the flow. These uncertainties were largely governed by sampling errors due to the finite number of measurements of concentration properties that were averaged at each point in the flow.

2.2.2. Velocity measurements

The PIV arrangement was similar to the arrangement used for the PLIF measurements except where noted. The arrangement consisted of a laser, optics for creating a laser sheet across the image area and a digital camera for recording the PIV images. Hollow glass spheres (8–12 μm in

diameter) were used to seed the source and ambient flow. The system uses a double pulse and frequency-doubled Nd:YAG laser (Spectra-Physics) to provide a beam at 532 nm (green) with roughly 10 ns pulse length. The beam is expanded into a parallel light sheet that intersects the vortical structure produced by the plume in the crossflow direction.

A mirror located roughly 1000 mm downstream from the imaged cross section of the flow allowed the camera to view the PIV images. These double-frame images were taken with a fast shuttered PIV camera (Cooke SensiCam SVGA, 1280×1024 pixels). The interrogation window size was set at 64×64 pixels and the interrogation window spacing was set at 10 pixels apart (there is overlap between neighboring interrogation windows). The magnification factor was 3.7 pixels/mm which gives roughly a 17×17 mm interrogation window size. The CCD chip in the camera has 1280×1024 pixels and the image consists of an array of 124×96 vectors (i.e., 11904 uniformly-spaced vectors). Some cropping of the field of view was required to remove the edge-effect of the mirror used in the water channel. Thus, the final PIV image consisted of 106×75 vectors.

The 532 nm green beam, with energies in excess of 100 mJ, was expanded into a laser sheet that crossed the test section perpendicular to the freestream flow. This laser sheet was approximately 1 mm thick and 40 cm wide. The time separation between the two pulses that provided the highest good-vector percentage was found to be 1 ms for this experiment. This time delay, as well as the laser Q-switches and flashlamps, were controlled by a Stanford Digital Delay Generator (DG 535). A programmable timing unit synchronizes the triggering of the lasers and camera.

Table 1
Summary of test conditions for steady round buoyant turbulent plumes in uniform crossflows

Property	Value
Source fluid	KH_2PO_4 and water
Crossflowing fluid	CH_3CH_2OH and water
Source mass solute (% by wt.)	3.6% KH_2PO_4
Crossflowing mass solute (% by wt.)	6.6% CH_3CH_2OH
Source dye conc. of Rhodamine 6G (μM)	5.0
Source fluid density (kg/m^3)	1024
Crossflowing fluid density (kg/m^3)	987
Index of refraction of source and ambient fluid	1.3372
Source fluid kinematic viscosity (mm^2/s)	1.05
Crossflowing fluid kinematic viscosity (mm^2/s)	1.33
Source diameter (mm)	2.1, 3.2 and 6.4
Source passage length, L/d	200, 100 and 50
Source flow rate (cc/s)	13–40
Source Froude number, $(\rho_0 u_0^2/(gd\Delta\rho))^{1/2}$	26–211
Source Reynolds number, $u_0 d/v_0$	5000–15,000
Source/crossflow fluid density ratio, ρ_0/ρ_∞	1.038
Source/crossflow fluid velocity ratio, u_0/v_∞	19–96
Streamwise (vertical) penetration distance, $(x_p - x_0)/d$	0–202
Cross stream (horizontal) penetration distance, $(y_p - y_0)/d$	0–380

The mean velocity fields were obtained over cross sections of the flow by averaging 1000 images. The experimental uncertainties (95% confidence) were less than 7% at each point in the flow. These uncertainties were largely governed by sampling errors due to the finite number of measurements of velocity properties that were averaged at each point in the flow.

2.3. Test conditions

Test conditions for the present experiments considering steady turbulent plumes in crossflow are summarized in Table 1.

3. Self-preserving structure properties

The present discussion of the self-preserving structure properties is limited to the behavior of jets in still fluids, as a baseline test for the PLIF technique, and steady turbulent plumes in crossflows (see Diez et al., 2003a,b) for consideration of the penetration properties of starting plumes in still and crossflowing fluids.

Analysis to find the self-preserving behavior of the mean and rms fluctuating concentration distributions in self-preserving steady round nonbuoyant turbulent jets in still fluids is well known (see List, 1982; Dahm and Dimotakis, 1990; Panchapakesan and Lumley, 1993, and references cited therein) for the details. The results of these analyses in terms of the present notation are as follows:

$$\bar{c}(x - x_{os})/(c_0 d) = F[r/(x - x_{os})], \tag{2}$$

$$(\bar{c}'/\bar{c}_m) = F'[r/(x - x_{os})], \tag{3}$$

where $\bar{c}_m$ is the maximum mean concentration of source fluid over the flow cross section (the maximum condition in the present case clearly is at the axis of the flow). This form of Eq. (3) for $\bar{c}'$ is used in order to simplify comparisons between present and earlier findings.

The configuration of the present steady turbulent plumes in crossflows considered in the following is sketched in Fig. 5. The source flow enters from a round passage normal to the crossflow and flows into an environment having a uniform crossflow velocity. As discussed by Diez et al. (2003a), the streamwise velocity decays rapidly with increasing streamwise distance for this flow; for example, the streamwise velocity is proportional to $(t - t_{os})^{-1/3}$ when the crossflow velocity is large compared to the streamwise velocity and the steady plume is nearly horizontal, as the self-preserving region is approached far from the source Diez et al., 2003a. In addition, the flow approximates no-slip convection in the cross stream direction Diez et al., 2003a,b. This behavior implies that the plume eventually is deflected so that its axis is nearly aligned with the cross stream direction. At this condition, the initial streamwise source specific buoyancy flux continues to be conserved so that the flow approximates the behavior of a line thermal. Then the streamwise source specific buoyancy flux per unit length of the line thermal causes a counter-rotating

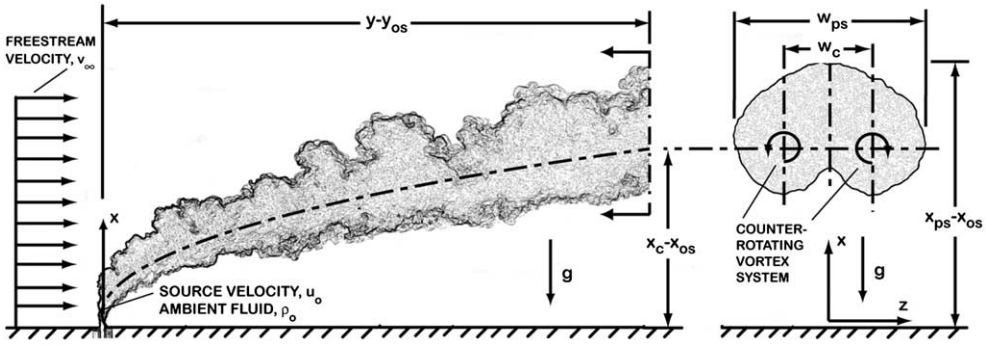

Fig. 5. Sketches of a steady turbulent plume in a uniform crossflow.

pair of vortices to form, leading to a somewhat flattened shape of the flow cross section. The streamwise source specific buoyancy flux per unit length can be expressed as follows:

$$B_0' = \dot{Q}_0 g|\rho_0 - \rho_\infty|/(\rho_\infty v_\infty). \tag{4}$$

Analyses to find the self-preserving behavior of the mean concentration distributions in self-preserving steady turbulent plumes in crossflows is described by Fischer et al. (1979). The results of these analyses in terms of the present notation are as follows:

$$\bar{c}g(x_c - x_{os})^2/(c_0 B_0') = F[(x - x_c)/(x_c - x_{os}), z/(x_c - x_{os})]. \tag{5}$$

Similarly, the analyses to find the self-preserving behavior of the mean *u*- and w-velocity distributions in self-preserving steady turbulent plumes in crossflows are described by Fischer et al. (1979). The results of these analyses in terms of the present notation are as follows:

$$\bar{u}(x_c - x_{os})^{1/2}/(B_0') = G[(x - x_c)/(x_c - x_{os}), z/(x_c - x_{os})], \tag{6}$$

$$\bar{w}(x_c - x_{os})^{1/2}/(B_0') = H[(x - x_c)/(x_c - x_{os}), z/(x_c - x_{os})]. \tag{7}$$

A similar analysis can be found in Hasselbrink and Mungal (2001a,b).

4. Results and discussion

4.1. Concentration measurements

Still fluids. In order to evaluate present PLIF measurements of concentration distributions over the cross section of steady round nonbuoyant turbulent plumes in uniform crossflows, initial measurements considered the well-studied case of a steady round constant-density turbulent jet in a still fluid.

The variation of radial profiles of mean concentrations as a function of streamwise distance from the jet exit is illustrated in Fig. 6. These results were obtained by averaging 4000 PLIF images at each streamwise station. The scaling parameters of Eq. (2) are used in this plot so that the ordinate is equal to $F(r/(x - x_{os}))$. The measurements are plotted for various streamwise distances with $(x - x_{os})/d \geqslant 12$. The maximum value of $(\bar{c}/c_0)(x - x_{os})/d)$ exhibits a progressive increase with increasing distance from the jet exit; this behavior is accompanied by a progressive narrowing of the flow in terms of the self-preserving scaled variables. However, self-preserving conditions are observed for present measurements when $(x - x_{os})/d \geqslant 32$. The subsequent variation of the profiles is well within the experimental uncertainties (95% confidence) of less than 10% for $(\bar{c}/\bar{c}_m)$ for $|r|/(x - x_0) < 0.2$ of the measurements over the range of the present experiments: $32 \leqslant (x - x_{os})/d \leqslant 400$, with jet exit Reynolds numbers in the range 5000–16,000. Within the self-preserving region, present radial profiles of mean mixture fractions are reasonably approximated by a Gaussian fit, similar to past work (e.g., Fischer et al., 1979; Law and Wang, 2000) as follows:

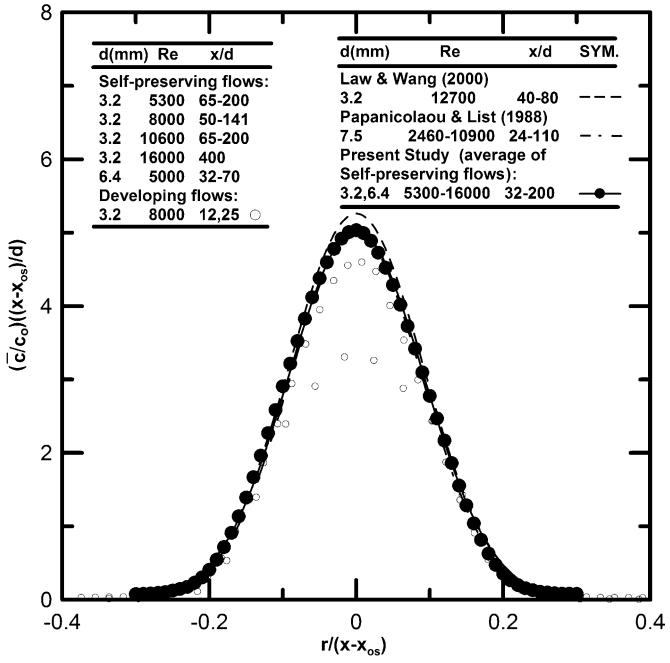

Fig. 6. Plots of mean concentrations of source fluid over the cross section of the flow in terms of self-preserving variables for steady round nonbuoyant turbulent jets in still environments.

$$F(r/(x-x_{os})) = F(0)\exp\{-k_c^2(r/(x-x_{os}))^2\}, \quad (8)$$

where

$$k_c = (x-x_{os})/\ell_c. \quad (9)$$

Thus, ℓ_c represents the characteristic jet radius where $\bar{c}/\bar{c}_c = \exp(-1)$. The best fit of the present measurements in the self-preserving region yielded $F(0) = 5.05$ and $k_c^2 = 59$. This correlation agrees with the findings of Dahm and Dimotakis (1990), based on measurements judged to be self-preserving in the range 100–350 source diameters from the source, within experimental uncertainties, helping to provide confidence in the present PLIF measurements. As can be seen from the results plotted in Fig. 6, present measurements of mean concentrations in the self-preserving region of steady round nonbuoyant turbulent jets in still fluids are also in good agreement with the earlier measurements of Law and Wang (2000), based on measurements in the range 40–80 source diameters from the source, and Fischer et al. (1979), based on measurements in the range 24–110 source diameters from the source.

Radial profiles of rms concentration fluctuations for streamwise distances of $(x-x_{os})/d$ of 32–400 are illustrated in Fig. 7; throughout this region, values of $\bar{c}'/\bar{c}_m$ exhibited self-preserving behavior for present measurements. Also shown on the plot are the earlier measurements of Papanicolaou and List (1988), based on measurements in the range 24–110 source diameters from the source, and Law and Wang (2000), based on measurements in the range 40–80 source diameters from the source, which are in qualitative agreement with the present measurements but exhibit significant amounts of scatter. All

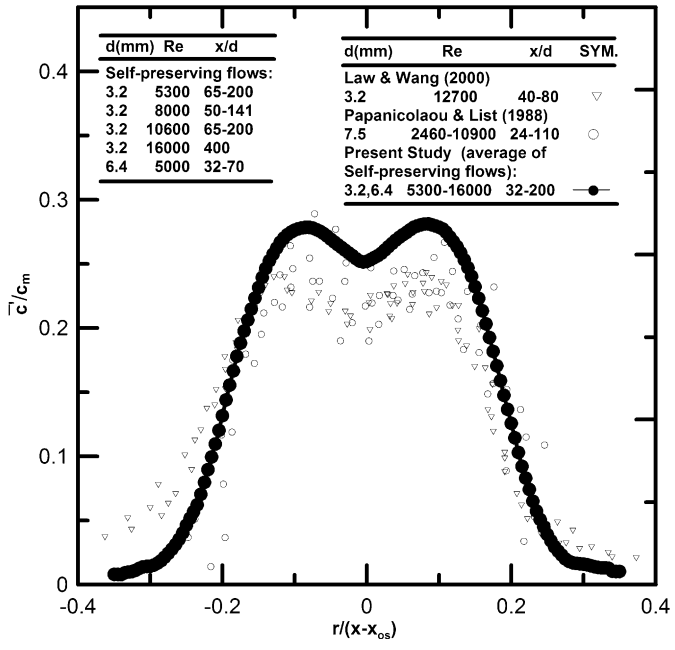

Fig. 7. Plots of rms concentration fluctuations of source fluid over the cross section of the flow in terms of self-preserving variables for steady round nonbuoyant turbulent jets in still environments.

these results have a dip in $\bar{c}'/\bar{c}_m$ near the axis which reflects reduced production of concentration fluctuations in this region because the radial gradient of $\bar{c}$ becomes small near the axis of the flow. Notably, round buoyant turbulent plumes in still environments do not exhibit a similar dip of concentration fluctuations near the axis because these flows undergo turbulence production near their axis due to the buoyant instability of the flow in this region—a mechanism that clearly is absent for the present nonbuoyant flows, see Dai et al. (1994) for plots of rms concentration fluctuations for steady round buoyant turbulent plumes in still environments.

To summarize, the baseline tests of present PLIF measurements for simple steady round nonbuoyant turbulent jets in still environments are in reasonably good qualitative and quantitative agreement with earlier measurements of this flow providing confidence in present PLIF measurements of flow structure.

Crossflow. The fine details of the dynamics of the mixing pattern of the source and ambient fluids in plumes in uniform crossflows can be seen from the sequence of PLIF images illustrated in Fig. 8. In order to achieve adequate spatial resolution for these PLIF images, the diameter of the laser beam sweeping the cross section of the flow was 0.5 mm. The time between images was 50 ms, which implies a cross stream distance between images that is relatively large compared to the integral length scales of the flow; therefore, the images illustrated in Fig. 8 are statistically independent. The instantaneous images appearing in Fig. 8 show the largely distorted presence of the two counter-rotating vortices separated near the plane of symmetry by the deeply-penetrating ambient fluid of the flow. In addition, the presence of ambient fluid being transported deep into the vortex system of the flow along its plane of symmetry clearly has an important effect on the flow structure, as mentioned earlier in connection with the discussion of the flow visualization of Fig. 1. The images in Fig. 8 show similar structures as those presented by Smith and Mungal (1998). In the other hand, the present images were taken in the self-preserving region of plumes in crossflow, as will be shown next, while Smith and Mungal (1998) mentioned that self-similarity was not seen in their ensemble-averaged images.

The distributions of mean concentrations over the cross section of steady turbulent plumes in crossflows in the self-preserving region are quite complex and cannot be reduced to a simple empirical formula similar to that obtained by Dai et al. (1994) for steady turbulent plumes in still fluids. Instead, present measurements of mean concentrations over cross sections in the self-preserving region were reduced in terms of self-preserving variables and plotted as a function of location in the cross section according to self-preserving streamwise and transverse variables indicated by Eq. (5), e.g., $(x-x_c)/(x_c-x_{os})$ and $z/(x_c-x_{os})$, respectively. Results of this nature are illustrated in Fig. 9 for the present test conditions from Table 1. The self-preserving scaled values of mean concentrations ranges

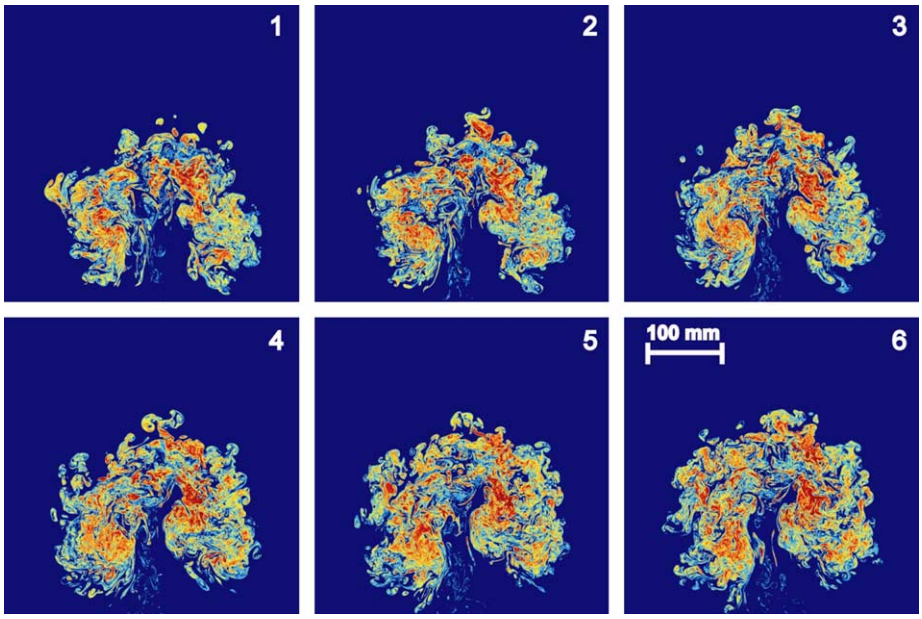

Fig. 8. Instantaneous PLIF images of the cross section of a steady turbulent plume in a uniform crossflow ($d = 3.2$ mm, $Re_0 = 15{,}000$, $\rho_0/\rho_\infty = 1.038$, $Fr_0 = 148$, $u_0/v_\infty = 44$, $(x_c - x_{os})/d = 108$, $y/d = 220$ and $\Delta t = 50$ ms between frames).

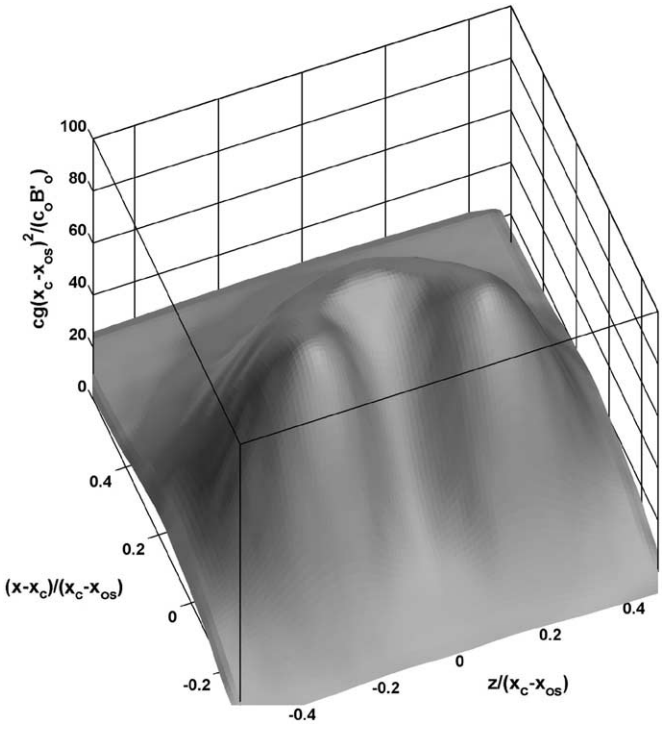

Fig. 9. Three-dimensional shaded surface of mean concentration profile of source fluid in terms of self-preserving variables over the cross section of the flow for steady turbulent plumes in crossflows within the self-preserving region.

from 0–70. The onset of self-preserving behavior required that the axes of the counter-rotating vortex system be nearly aligned with the crossflow direction. This alignment, in turn, was a strong function of the source/crossflow velocity ratio, u_0/v_∞. The net result was that the onset of self-preserving behavior was observed at streamwise distances of 10–20 source diameters from the source for $u_0/v_\infty = 4$, increasing to streamwise distances of 160–170 source diameters from the source for $u_0/v_\infty = 100$. The counter-rotating vortex system is seen to contribute to the two-lobed structure of the flow with the entrainment of ambient fluid along the plane of symmetry from the side of the flow opposite to the plume source tending to displace maximum mean concentrations along this plane in the streamwise (upward) direction (i.e., in the direction of penetration of the counter-rotating vortex system). A particularly surprising feature of this flow is its unusually large streamwise and transverse penetration distances of $(x - x_c)/(x_c - x_{os})$ of approximately $+0.6$ to -0.3 and $z/(x_c - x_{os})$ of approximately ± 0.5. These values are 2–3 times larger than the corresponding radial dimensions of steady round buoyant turbulent plumes in still fluids, see Dai et al. (1994), where $r/(x - x_0)$ is approximately 0.16. In addition, the concentration field for steady turbulent plumes in crossflows decays according to $\bar{c}_m \sim (x - x_{os})^{-2}$, which is slightly faster than for steady turbulent plumes in still fluids which decays according to $\bar{c}_m \sim (x - x_{os})^{-5/3}$ Dai et al., 1994. This highlights the capability of vortex structures in crossflow to promote effective mixing between source and ambient fluids.

4.2. Velocity measurements

The fine details of a typical instantaneous velocity and vorticity fields of a cross section of a steady turbulent plume in a uniform crossflow are shown in a velocity vector plot and vorticity contour plot, respectively in Fig. 10. In Fig. 11 the mean concentrations of source fluid and veloc-

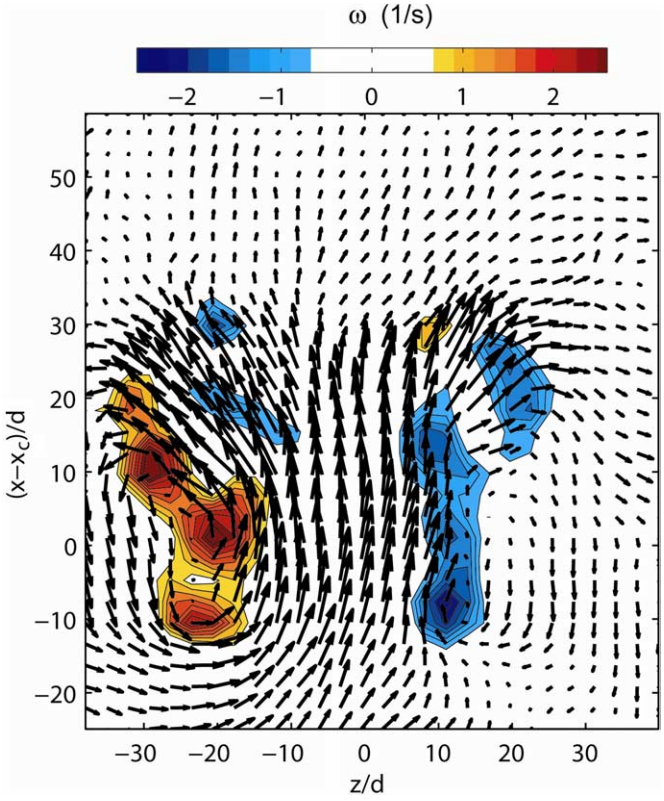

Fig. 10. Instantaneous velocity vector plot from PIV measurements and instantaneous vorticity contour plot of the cross section of a steady turbulent plume in a uniform crossflow ($d = 3.2$ mm, $Re_0 = 9000$, $\rho_0/\rho_\infty = 1.038$, $Fr_0 = 88$, $u_0/v_\infty = 37$, $y/d = 220$).

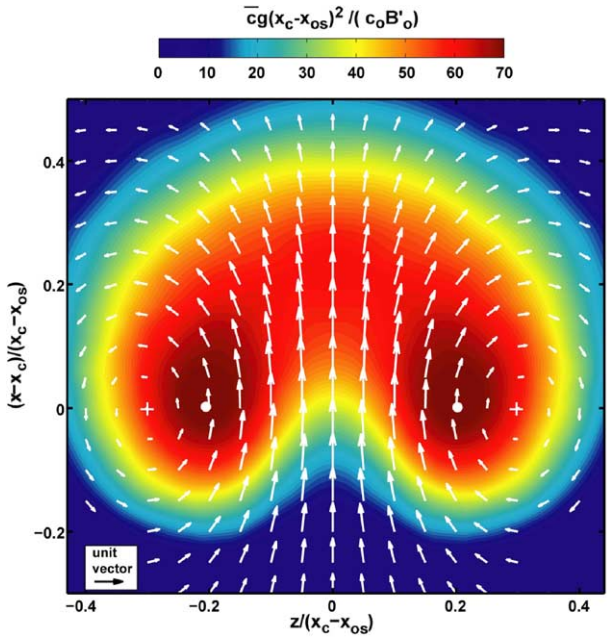

Fig. 11. Contour plots of mean concentrations of source fluid and velocity vector plot in terms of self-preserving variables over the cross section of the flow for steady turbulent plumes in crossflows within the self-preserving region.

ity vector distribution are superimposed and plotted according to the self-preserving structure variables of Eqs. (5)–(7). The counter-rotating vortex system is clearly observed both in the mean concentration and velocity vector plots. The centers of rotation of the counter-rotating vortex system are shown as white crosses on these plots, and the centers of maximum mean concentration of the counter-rotating vortex system are shown as white dots on these plots, for reference purposes. A particularly surprising feature of this flow is how far the centers of rotation of the counter-rotating vortex system are ($z/(x_c - x_{os})$ of approximately ± 0.3) in comparison with the location of the centers of maximum mean concentration of the counter-rotating vortex system ($z/(x_c - x_{os})$ of approximately ± 0.2).

5. Conclusions

Scaling relationships for the structure properties of steady turbulent plumes in crossflows were evaluated based on measurements of the mixing properties of salt water sources injected into ethanol/water crossflows. Major conclusions of the study are as follows:

(1) Measurements of the mean concentration of source fluid and mean velocity fields were obtained for the first time in the self-preserving region of steady round buoyant turbulent plumes. These challenging measurements included the use of refractive index matching in order to remove refractive index variations in the mixing flow from density changes. Also, in order to achieve accurate results, the individual images were corrected for vignetting, sweep geometry, attenuation (by water, Rhodamine 6G, sodium phosphate and ethanol) and background effects.

(2) The self-preserving structure of steady turbulent plumes in crossflows involves a counter-rotating vortex system whose axes is nearly aligned with the crossflow and thus is nearly horizontal. The nearly crossflow orientation of the axes of the counter-rotating vortex system promotes unusually rapid mixing due to the approximately crossflow motion in the streamwise direction of steady turbulent plumes in crossflows compared to steady turbulent plumes in still fluids where the flow axis is aligned with the streamwise direction, for example: (r_{ps} and w_{ps})/($x_{ps} - x_{os}$) = 0.36 and 0.49 for steady turbulent plumes in crossflow compared to $r_p/(x_p - x_{os}) = 0.16$ for steady turbulent plumes in still fluids.

Acknowledgements

This research was supported by the United States Department of Commerce, National Institute of Standards and Technology (NIST), Grant No. 60NANB1D0006, with H.R. Baum of the Building and Fire Research Labo-

ratory serving as Scientific Officer. The assistance of D. Zoch and R. Jolly in carrying out the experiments is gratefully acknowledged.

References

Alahyari, A., Longmire, E.K., 1994. Particle image velocimetry in a variable density flow: application to dynamically evolving microburst. Exp. Fluids 17, 434–440.

Alton, B.W., Davidson, G.A., Slawson, P.R., 1993. Comparison of measurements and integral model predictions of hot water plume behavior in a crossflow. Atmos. Environ. Part A 27A, 589–598.

Andreopoulos, J., 1983. Heat transfer measurements in a heated jet-pipe flow issuing into a cold cross stream. Phys. Fluids 26, 3200–3210.

Baum, H.R., McGrattan, K.B., Rehm, R.G., 1994. Simulation of smoke plumes from large pool fires. Proc. Combust. Inst. 25, 1463–1469.

Dahm, W.J.A., Dimotakis, P.E., 1990. Mixing at large schmidt number in the self-similar far field of turbulent jets. J. Fluid Mech. 217, 299–330.

Dai, Z., Tseng, L.-K., Faeth, G.M., 1994. Structure of round, fully-developed, buoyant turbulent plumes. ASME J. Heat Trans. 116, 409–417.

Daviero, G.I., Roberts, P.J.W., Maile, K., 2001. Refractive index matching in large-scale stratified experiments. Exp. Fluids 31, 119–126.

Diez, F.J., Bernal, L.P., Faeth, G.M., 2003a. Round turbulent thermals, puffs, starting plumes and starting jets in uniform crossflow. ASME J. Heat Trans. 125, 1046–1057.

Diez, F.J., Sangras, R., Faeth, G.M., Kwon, O.C., 2003b. Self-preserving properties of unsteady round turbulent plumes and thermals in still fluids. ASME J. Heat Trans. 125, 821–830.

Diez, F.J., Sangras, R., Kwon, O.C., Faeth, G.M., 2003c. Self-preserving properties of unsteady round nonbuoyuant turbulent starting jets and puffs in still fluids. ASME J. Heat Trans. 125, 204–205.

Diez, F.J., Bernal, L.P., Faeth, G.M., 2005. Self-preserving mixing properties of steady round nonbuoyant turbulent jets in uniform crossflows. ASME J. Heat Trans. 127, 877–887.

Ferrier, A.J., Funk, D.R., Roberts, P.J.W., 1993. Application of optical techniques to the study of plumes in stratified fluids. Dyn. Atmos. Oceans 20, 155–183.

Fischer, H.B., List, E.J., Koh, R.C., Imberger, J., Brooks, N.H., 1979. Mixing in Inland and Coastal Waters. Academic Press, New York, pp. 315–389.

Gordon, M., Soria, J., 2001. PIV measurements of a zero-net-mass-flux jet in cross flow. Exp. Fluids 33, 863–872.

Hasselbrink Jr., E.F., Mungal, M.G., 2001a. Transverse jets and jet flames. Part. 1. Scaling laws for strong transverse jets. J. Fluid Mech. 443, 1–25.

Hasselbrink Jr., E.F., Mungal, M.G., 2001b. Transverse jets and jet flames. Part 2. Velocity and OH field imaging. J. Fluid Mech. 443, 27–68.

Hinze, J.O., 1975, second ed. McGraw-Hill, New York, pp. 534–585.

Johari, J., Paduano, R., 1987. Dilution and mixing in an unsteady turbulent jet. Exp. Fluids 23, 272–280.

Kato, S.M., Groenwagen, B.C., Breidenthal, R.E., 1987. On turbulent mixing in nonsteady jets. AIAA J. 25, 165–168.

Kouros, H., Medina, R., Johari, H., 1993. Spreading rate of an unsteady turbulent jet. AIAA J. 31, 1524–1526.

Law, A.W.-K., Wang, H., 2000. Measurement of mixing processes with combined digital particle image velocimetry and planar laser induced fluorescence. Exp. Therm. Fluid Sci. 22, 213–229.

List, E.J., 1982. Turbulent jets and plumes. Ann. Rev. Fluid Mech. 14, 189–212.

Lutti, F.M., Brzustowski, T.A., 1977. Flow due to a two-dimensional heat source with cross flow in the atmosphere combust. Sci. Tech. 16, 71–87.

Mi, J., Nobes, D.S., Nathan, G.J., 2001. Influence of jet exit conditions on the passive scalar field on an axisymmetric free jet. J. Fluid Mech. 10, 91–125.

Panchapakesan, N.R., Lumley, J.L., 1993. Turbulence measurements in axisymmetric jets of air and helium. Part 1. Air jet. J. Fluid Mech. 246, 197–223.

Papanicolaou, P.N., List, C.J., 1988. Investigation of round vertical turbulent buoyant jets. J. Fluid Mech. 95, 151–190.

Sangras, R., Kwon, O.C., Faeth, G.M., 2002. Self-preserving properties of unsteady round nonbuoyant turbulent starting jets and puffs in still fluidzs. ASME J. Heat Trans. 124, 460–469.

Smith, S.H., Mungal, M.G., 1998. Mixing, structure and scaling of the jet in crossflow. J. Fluid Mech. 357, 83–122.

Steckler, K.D., Baum, H.R., Quintiere, J.G., 1986. Salt water modeling of fire induced flows in multicomponent enclosures. Proc. Combust. Inst. 21, 143–149.

Su, L.K., Mungal, M.G., 2004. Simultaneous measurements of scalar and velocity field evolution in turbulent crossflowing jets. J. Fluid Mech. 513, 1–45.

Tennekes, H., Lumley, J.L., 1972. A First Course in Turbulence. MIT Press, Cambridge, Massachusetts, pp. 113–124.

Wu, P.-K., Miranda, R.F., Faeth, G.M., 1995. Effects of initial flow conditions on primary breakup of nonturbulent and turbulent round liquid jets. Atom. Sprays 5, 175–196.